



Analysis of sublimation growth of bulk SiC crystals in tantalum container

S.Yu. Karpov^a, A.V. Kulik^a, I.A. Zhmakin^a, Yu.N. Makarov^b, E.N. Mokhov^c,
M.G. Ramm^c, M.S. Ramm^{c,*}, A.D. Roenkov^c, Yu.A. Vodakov^c

^a*Soft-Impact Limited, P.O. Box 33, 194156 St. Petersburg, Russia*

^b*Fluid Mechanics Department, University of Erlangen-Nürnberg, Cauerstrasse 4, D-91058 Erlangen, Germany*

^c*A.F. Ioffe Physical Technical Institute, Russian Academy of Sciences, Polytechnicheskaya 26, 194021 St. Petersburg, Russia*

Abstract

Sublimation growth of SiC bulk crystals in tantalum container is studied both experimentally and theoretically. The model of heterogeneous processes occurred on the side wall of the tantalum container proposed recently in Ramm et al. (Mat. Sci. Eng. B 61–62 (1999) 107) is extended to take into account the process of carbon gettering by the container side wall. We formulate a quasi-steady approach for modeling of the bulk crystal growth. Using this concept we predict evolution of the crystal shape and study processes which govern SiC bulk crystal growth. We apply anisotropic thermal elastic analysis to predict stress distribution in the growing crystal. For the first time a model of dislocation formation is applied for SiC bulk growth to compute dislocation density field in highly stressed areas of the growing crystal. © 2000 Published by Elsevier Science B.V. All rights reserved.

Keywords: SiC; Bulk crystal growth; Sublimation; Tantalum; Thermoelastic analysis; Dislocation density

1. Introduction

Sublimation growth of SiC bulk crystals in tantalum container is a promising method to obtain wafers with low density of micropipes and other structural defects [1,2]. The effect of tantalum container on growth rate and vapor-phase composition was discussed earlier in Refs. [2–4]. In Ref. [1] comparison of graphite and tantalum growth systems was carried out by numerical modeling using a simplified model of heterogeneous processes occurring on the side wall of the tantalum container.

This led to the understanding of a number of specific features of tantalum system compared to the graphite one. Nevertheless, some peculiarities of SiC growth in the tantalum container (particularly, gettering of carbon by Ta side walls) mentioned in Ref. [2] were not previously considered. In this work, the model of SiC growth in tantalum container introduced in Ref. [1] is further developed to account for the gettering effect. Using this extended model we investigate evolution of SiC crystal shape and study effects of the process parameters critical for control of the crystallization front profile. Modeling of SiC bulk crystal growth is coupled with analysis of thermoelastic strain resulting in the appearance of dislocations in the volume of the crystal.

* Corresponding author.

E-mail address: ramm@model.ioffe.rssi.ru (M.S. Ramm)

2. Heterogeneous processes on the side wall of tantalum container

Special experiments were carried out to estimate the rate of carbon gettering by the container wall. For this purpose we annealed the container in the atmosphere of Si–C vapors at high temperature. It was known that such procedure leads to partial transformation of tantalum into TaC [2]. Thus, the increase of container weight after annealing was associated with carbon gettering. Weight increment was used to estimate the gettering rate J_0 , i.e. a number of carbon atoms incorporated into the wall of the container at the unit area of per unit time. The gettering rate was found to depend on temperature and thickness of the tantalum container.

In our computations we take into account both carbon gettering and heterogeneous reactions, occurring on the container side wall. Geometry of the growth system is chosen close to that considered in Ref. [1]. Our analysis shows that carbon gettering results in minor (by $\sim 10\%$) decrease of SiC growth rate. This is related to decreasing of total amount of carbon in the vapor phase (due to gettering) which limits the growth rate of the crystal. In addition, the Si/C ratio over the seed surface rises. This means that carbon gettering leads to enrichment of the vapor phase by silicon that is favorable for suppression of graphitization of the seed surface and the SiC powder source. These conclusions agree well with experimental observations.

3. Evolution of SiC crystal and of the source during sublimation growth

Growth of SiC bulk crystal is a non-steady-state process. First, the inductor coil used for heating of the container is usually moved during the growth to provide the necessary temperature of the seed and temperature gradient between the surfaces of the seed and source. As a rule, the coil velocity is varied in time. Second, during SiC growth the crystal shape changes, SiC source sublimates and the volume of the SiC powder charge is decreasing. All these factors result in gradual change of SiC growth rate. Properties of the SiC powder (porosity and composition) and surface profile of the charge are

also continuously changing during the growth process that was experimentally observed in Ref. [5].

Specific transient times related to the changes of thermal boundary conditions and geometry of the growth cell are much less than the duration of the growth process as a whole. Consequently, a steady-state approach can be applied for every stage of the growth to simulate heat and mass transport in the system. We study evolution of SiC crystal by dividing the process duration t_{gr} into n steps (duration of each step is τ , $t_{gr} = n \cdot \tau$) and simulating SiC growth at every step, taking into account variation of the growth conditions from step to step. At each step we solve the coupled two-dimensional heat [6] and mass transport equations to obtain SiC growth rate at the seed V_{gr} and sublimation rate at the source surface V_{subl} . The species transport inside the container is described by the Navier–Stokes equations reduced for low Mach number multicomponent flows [7]. The equations are added by a set of boundary conditions accounting for heterogeneous chemical reactions at the solid–gas interfaces [1,6]. The obtained values of V_{gr} and V_{subl} are used then to recalculate the location of the crystallization front and of the powder charge surface at the end of the growth step.

Growth system geometry used in the computations is shown schematically in Fig. 1. Evolution of the crystal shape and of the profile of SiC powder surface is displayed in Fig. 2. The highest temperatures in the growth system are observed in the volume of the powder charge near the container side wall. This causes efficient sublimation of the powder near the wall and results in a lowering of the surface of the powder charge. In turn, this effect leads to the movement of sublimation front towards the area of higher temperature. As a result, the sublimation rate at the periphery of the source surface increases in time.

Evolution of the crystal shape (see Fig. 2) is a much more complicated process. The growth rate profile is controlled not only by temperature distribution over the growth container but also by species transport from the source to the crystal and their chemical interactions with the side wall of the container. The modeling results show that at the initial stages of the growth process the growth rate

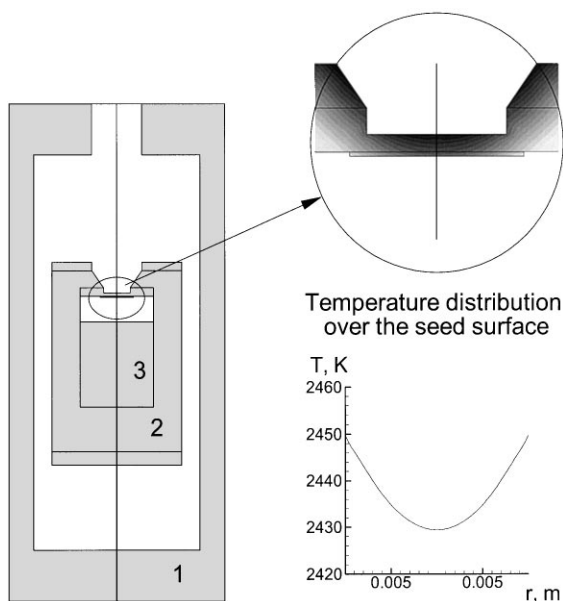


Fig. 1. Scheme of the growth system: (1) graphite foam, (2) tantalum container, (3) SiC powder charge. The upper inset shows the part of the container near the seed. One-dimensional temperature distribution over the seed surface at the initial stage of the growth is shown in the lower inset.

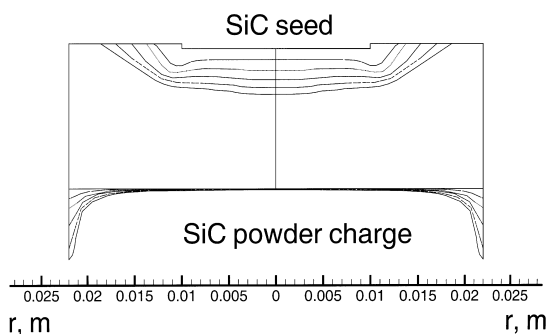


Fig. 2. Evolution of the crystal shape and the surface of the powder charge (time step $\tau = 4$ h). Movement of the inductor coil position $z_c(t)$ is set as $z_c(t) = 0$ at $t < 4$ h and $z_c(t) = 2.5(t - 4)$ at $t > 4$ h ($[t] = \text{h}$, $[z_c] = \text{mm}$).

is higher at the seed edge in spite of the fact that minimal temperature is at the center of the seed (see Fig. 1). In the beginning, the growth is more than twice as large as that at the center of the crystal. This is due to the two-dimensional character of the

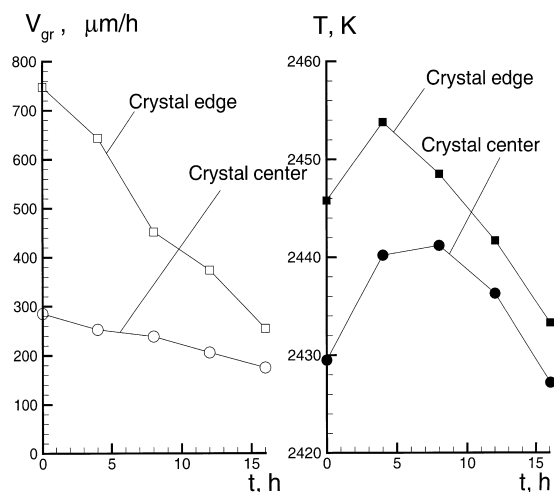


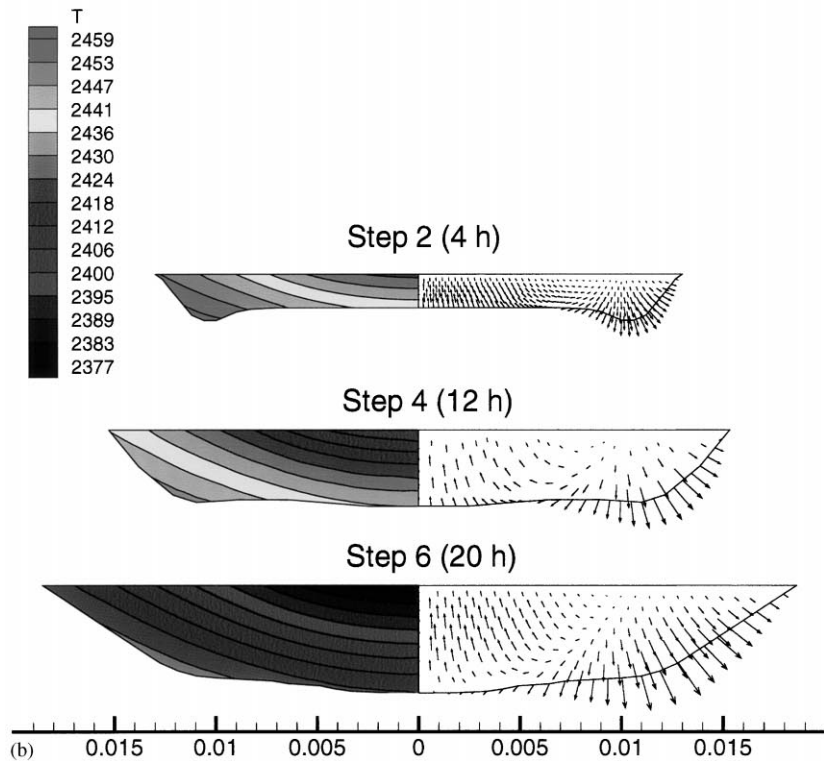
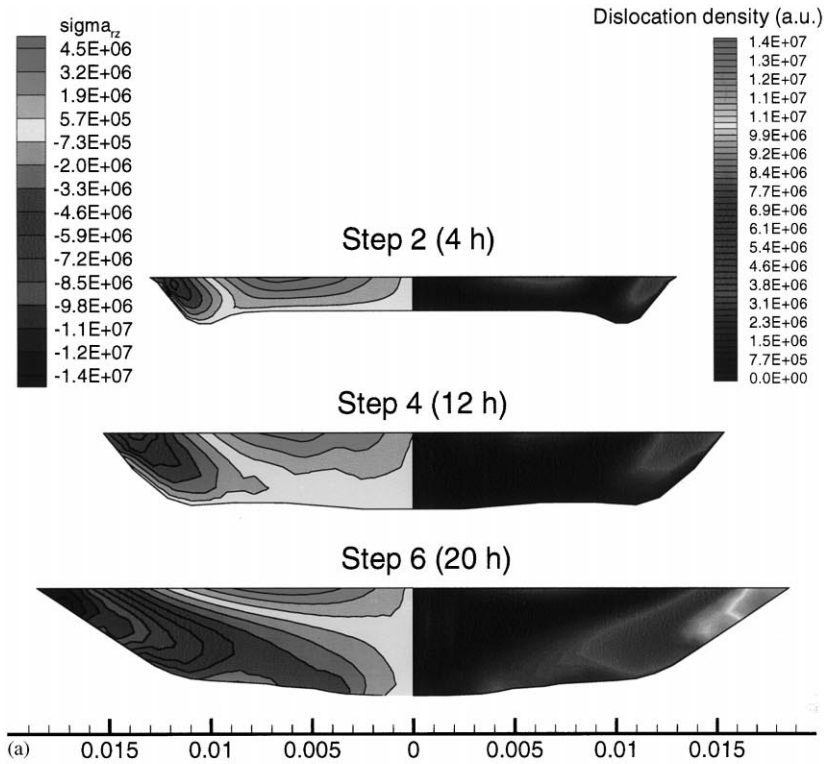
Fig. 3. Evolution of the growth rate (left) and of the temperature (right) at the center (circles) and at the periphery (squares) of the crystal.

species transport from the source to the seed and predominant sublimation of the source at the periphery. Fig. 3 shows that at the later stages of the growth process the crystal shape becomes more flat due to significant decrease of the growth rate at the periphery of the crystal compared to that at the center. The evolution of the shape of the crystal predicted in our calculations agrees qualitatively with experimental observations.

It should be noted specially that only thermal calculations are not definitely sufficient to predict evolution of the shape of the growing crystal and can misguide crystal grower. Our analysis demonstrates clearly that prediction of the shape of the crystallization front requires coupled two-dimensional heat and mass transport calculations.

4. Analysis of thermoelastic stress

Important issue in SiC bulk crystal growth is formation of dislocations due to thermoelastic strain arisen from non-uniform temperature distribution inside the crystal. To predict qualitatively the dislocation density we use the anisotropic elasticity theory to calculate the thermoelastic strain in SiC crystal at each step of the growth. Fig. 4(b)



shows evolution of temperature distribution and corresponding displacement vectors in the growing crystal. One can see that despite of the weak temperature variation inside the crystal, the displacement field is significantly non-uniform. The computed thermoelastic stress is then used for estimation of density of dislocations appeared during growth of SiC crystal. For this purpose we assume that the basal (0 0 0 1) plane is the principal gliding plane for generated dislocations [8]. Following Jordan et al. [9] we accept that dislocations appearance results in full strain relaxation while thermoelastic shear stress exceeding the plasticity threshold σ_{cr} associated with the gliding plane of the crystal. In this case density of dislocations should be proportional to the value of $(|\sigma_{rz}| - \sigma_{cr})$ [9].

In the computations we used temperature-dependent value of σ_{cr} . This value was obtained by approximation of the experimental data of Ref. [8] corresponding to the slowest rate of shear stress generation in SiC crystal. It is found that the critical resolved shear stress as a function of temperature can be well fitted by the Arrhenius curve. Extrapolation of this curve into growth temperature range results in the value of $\sigma_{cr} = 9.0 \times 10^5$ Pa at $T = 2500$ K. The dimensionless dislocation density $(|\sigma_{rz}| - \sigma_{cr})$ obtained by such a way and σ_{rz} field are shown in Fig. 4(a). These results are obtained assuming strict fixation of the crystal at the upper wall of the container (both components of the displacement vector are equal here to zero). That is why the dislocation density obtained in our computations can be somewhat overestimated as compared to practical situation. Nevertheless, the theory predicts reasonably well predominant appearance of the dislocations near the crystal edges.

5. Summary

In this paper we extended the model of sublimation process in tantalum container accounting for

carbon gettering by the container side wall. The proposed approach allowed us to simulate the bulk SiC crystal growth at different stages and to trace the crystal shape evolution. For the first time the theoretical prediction of dislocation density evolution during SiC growth is performed.

Use of combined modeling and experimental process optimization allowed us to obtain SiC crystals up to 25–30 mm in diameter with micropipe density lower than 30 cm^{-2} . For the best crystals the density at a rate of several micropipes per square centimeter was reached. The source utilization efficiency higher than 90% was achieved.

References

- [1] M.S. Ramm, E.N. Mokhov, S.E. Demina, M.G. Ramm, A.D. Roenkov, Yu.A. Vodakov, A.S. Segal, A.N. Vorob'ev, S.Yu. Karpov, A.V. Kulik, Yu.N. Makarov, *Mat. Sci. Eng. B* 61–62 (1999) 107.
- [2] Yu.A. Vodakov, A.D. Roenkov, M.G. Ramm, E.N. Mokhov, Yu.N. Makarov, *Phys. Stat. Sol.* 202 (1997) 177.
- [3] D. Hoffman, S.Yu. Karpov, Yu.N. Makarov, E.N. Mokhov, M.G. Ramm, M.S. Ramm, A.D. Roenkov, Yu.A. Vodakov, *Inst. Phys. Conf. Ser.* 142 (1996) 29.
- [4] D. Hoffman, S.Yu. Karpov, Yu.N. Makarov, E.N. Mokhov, M.G. Ramm, M.S. Ramm, A.D. Roenkov, Yu.A. Vodakov, *Abstracts of E-MRS Spring Meeting* (1996) A-16.
- [5] D. Hoffman, M. Bickermann, R. Eckstein, M. Kölbl, St.G. Müller, E. Schmitt, A. Weber, A. Winnacker, *J. Crystal Growth* 198/199 (1999) 1005.
- [6] Yu.E. Egorov, A.O. Galyukov, S.G. Gurevich, Yu.N. Makarov, E.N. Mokhov, M.G. Ramm, M.S. Ramm, A.D. Roenkov, A.S. Segal, Yu.A. Vodakov, A.N. Vorob'ev, A.I. Zhmakin, *Mater. Sci. Forum* 264–268 (1998) 61.
- [7] Yu.N. Makarov, A.I. Zhmakin, *J. Crystal Growth* 94 (1989) 537.
- [8] A.V. Samant, W.L. Zhou, P. Pirouz, *Mater. Sci. Forum* 264–268 (1998) 627.
- [9] A.S. Jordan, R. Caruso, A.R. VonNeida, J.W. Nielsen, *J. Appl. Phys.* 52 (5) (1981) 3331.

Fig. 4. (a) Evolution of the shear stress σ_{rz} and of the dimensionless dislocation density in the growing crystal. (b) Evolution of temperature field (left), and of the displacement vectors in the growing crystal due to thermoelastic strain.